



Artificial intelligence-based detection of lymph node metastases by PET/CT predicts prostate cancer-specific survival

Downloaded from: <https://research.chalmers.se>, 2024-07-27 03:13 UTC

Citation for the original published paper (version of record):

Borrelli, P., Larsson, M., Ulen, J. et al (2021). Artificial intelligence-based detection of lymph node metastases by PET/CT predicts prostate cancer-specific survival. *Clinical Physiology and Functional Imaging*, 41(1): 62-67.
<http://dx.doi.org/10.1111/cpf.12666>

N.B. When citing this work, cite the original published paper.



Artificial intelligence-based detection of lymph node metastases by PET/CT predicts prostate cancer-specific survival

Pablo Borrelli¹ | Måns Larsson^{2,3} | Johannes Ulén³ | Olof Enqvist^{2,3} |
Elin Trägårdh⁴ | Mads Hvid Poulsen^{5,6} | Mike Allan Mortensen⁵ |
Henrik Kjölhede^{7,8} | Poul Flemming Høilund-Carlsen^{6,9} | Lars Edenbrandt^{1,10}

¹Department of Clinical Physiology, Region Västra Götaland, Sahlgrenska University Hospital, Gothenburg, Sweden

²Department of Electrical Engineering, Chalmers University of Technology, Gothenburg, Sweden

³Eigenvision AB, Malmö, Sweden

⁴Department of Clinical Physiology and Nuclear Medicine, Lund University and Skåne University Hospital, Malmö, Sweden

⁵Department of Urology, Odense University Hospital, Odense, Denmark

⁶Department of Clinical Research, University of Southern Denmark, Odense, Denmark

⁷Department of Urology, Region Västra Götaland, Sahlgrenska University Hospital, Gothenburg, Sweden

⁸Department of Urology, Institute of Clinical Science, Sahlgrenska Academy, University of Gothenburg, Gothenburg, Sweden

⁹Department of Nuclear Medicine, Odense University Hospital, Odense, Denmark

¹⁰Department of Molecular and Clinical Medicine, Institute of Medicine, Sahlgrenska Academy, University of Gothenburg, Gothenburg, Sweden

Correspondence

Pablo Borrelli, Department of Clinical Physiology, Region Västra Götaland, Sahlgrenska University Hospital, Gothenburg, Sweden.
Email: pablo.borrelli@vregion.se

Funding information

Sveriges Regering, Grant/Award Number: ALFGBG-720751; EXINI Diagnostics AB

Abstract

Introduction: Lymph node metastases are a key prognostic factor in prostate cancer (PCa), but detecting lymph node lesions from PET/CT images is a subjective process resulting in inter-reader variability. Artificial intelligence (AI)-based methods can provide an objective image analysis. We aimed at developing and validating an AI-based tool for detection of lymph node lesions.

Methods: A group of 399 patients with biopsy-proven PCa who had undergone ¹⁸F-choline PET/CT for staging prior to treatment were used to train ($n = 319$) and test ($n = 80$) the AI-based tool. The tool consisted of convolutional neural networks using complete PET/CT scans as inputs. In the test set, the AI-based lymph node detections were compared to those of two independent readers. The association with PCa-specific survival was investigated.

Results: The AI-based tool detected more lymph node lesions than Reader B (98 vs. 87/117; $p = .045$) using Reader A as reference. AI-based tool and Reader A showed similar performance (90 vs. 87/111; $p = .63$) using Reader B as reference. The number of lymph node lesions detected by the AI-based tool, PSA, and curative treatment was significantly associated with PCa-specific survival.

Conclusion: This study shows the feasibility of using an AI-based tool for automated and objective interpretation of PET/CT images that can provide assessments of lymph node lesions comparable with that of experienced readers and prognostic information in PCa patients.

KEYWORDS

artificial intelligence, fluorocholine, lymph node metastases, PCa, PET

1 | INTRODUCTION

Detecting lymph node metastases is important for staging patients with newly diagnosed prostate cancer (PCa) and for managing patients with biochemically recurrent PCa. Reading PET/CT images is a subjective process, and the degree of experience and knowledge varies among physicians. Standards for reporting PCa molecular imaging have been proposed as a way to reduce the consequent variability both in clinical reporting and research (Eiber et al., 2018; Fendler et al., 2017). Alternatively, artificial intelligence (AI)-based methods can provide a quantitative assessment within seconds with reduced variability and high reproducibility, allowing more objective reporting. One such example is the bone scan index, which is an AI-based method offering an imaging biomarker that reflects the skeletal tumour burden in a reproducible way. In a large phase 3 multicentre clinical trial, this index has been shown to be an independent prognostic biomarker of survival in metastatic castration-resistant PCa (Armstrong et al., 2018).

In recent years, convolutional neural networks (CNNs) have revolutionized the field of image analysis. The vision is that AI methods applied to whole-body PET/CT scans can provide a single number, the global disease score, to reflect the entire disease burden in the body or part of the body (Høilund-Carlsen et al., 2019). We have used CNNs to automatically detect and quantify PET tracer activity in the prostate gland and skeleton of patients with PCa (Lindgren Belal et al., 2017; Polymeri et al., 2020). Both methods provided volumetric measurements of tumour burden, which is associated with overall survival. An additional step towards a faster and comprehensive automated analysis that provides a global disease score in PCa patients is the detection and quantification of lymph node metastases. The challenge with lymph node detection compared to lesions in the prostate gland or skeleton is that the lymph nodes are not limited to an organ that can be segmented from the CT scan. Furthermore, the number of false positives that contain non-specific physiological radiotracer uptake and have a similar appearance is considerably larger and should be kept as low as possible without hampering sensitivity.

The aim of the present study was to explore the feasibility of using CNNs to detect lymph node metastases with PET/CT imaging in PCa patients. A secondary aim was to investigate the association between the number of automatically detected lymph node metastases and PCa-specific survival.

2 | MATERIALS AND METHODS

The AI-based tool consisted of two CNNs, the Detection CNN trained to detect lymph node lesions and the Organ CNN (Trägårdh et al., 2020) trained to segment organs. To classify an area of high tracer uptake as a lymph node lesion is, to a great extent, a question of ruling out any other explanation, for example, high uptake reflecting normal uptake in the kidneys, liver, prostate or urinary bladder. Hence, a mask of the organs segmented by the Organ CNN was used

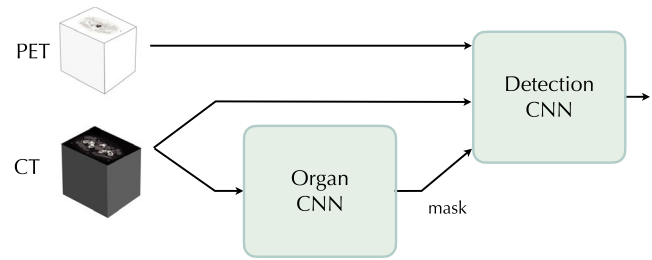


FIGURE 1 Schematic design of the AI-based tool. There are three inputs to the Detection CNN: the PET image, the CT image and an organ mask generated by the Organ CNN (Convolutional Neural Network)

as an auxiliary input to the Detection CNN (Figure 1). We examined this in a retrospective analysis of three patient cohorts all studied with ^{18}F -choline.

2.1 | Patients

The Detection CNN was trained and tested with PET/CT scans from 399 patients with biopsy-proven PCa. The PET/CT scans were obtained for staging prior to treatment (androgen deprivation, radical prostatectomy or radiation therapy). The PCa patients had a median age of 69 years (range 42–89) and a median PSA of 21 ng/ml (range 1.4–2,970). The Gleason score was six or less in 18 patients, seven in 145 patients, and eight or higher in 231 patients (missing data from five patients). A total of 279 PCa patients underwent curative treatment after PET/CT. The patients were retrospectively included from three prior studies focusing on PET/CT imaging in PCa; 42 patients from a study by Poulsen et al. (2014) at the Odense University Hospital in Denmark between March 2010 and May 2014; 399 patients from a study by Kjölhede et al. (2018) at the Skåne University Hospital in Sweden between February 2008 and November 2011; 50 patients from a study by Mortensen et al. (2019) at the Odense University Hospital in Denmark between January 2013 and April 2014. The patients were randomly divided into a training group (319 patients; 80%) and a test group (80 patients; 20%).

The Organ CNN was trained on a separate group of 225 patients referred for PET/CT with known or suspected cancer other than PCa. Only the CT scans were used in the training process. The training group for the Organ CNN came from the Sahlgrenska University Hospital in Sweden.

2.2 | Ethics statement

All procedures performed in studies involving human participants were in accordance with the ethical standards of the institutional and/or national research committee (ethical approval was obtained from the Regional Ethical Review Boards at Lund University (LU552/2007; Lindgren Belal et al., 2017), Gothenburg University

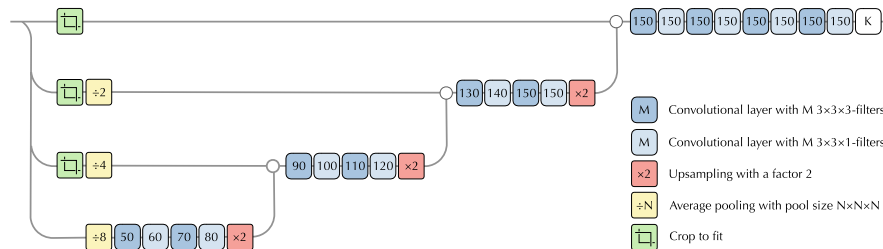


FIGURE 2 The structure of the convolutional neural network used both for the Organ CNN and the Detection CNN. Blue boxes are $3 \times 3 \times 3$ convolutional layers, and the number indicates the number of filters. Red boxes are $2 \times$ -upsampling layers, and yellow boxes are average pooling, where the number indicates the pool size. The effect of the pooling layers is that the network works on four different resolutions. This allows for a large receptive field with low memory cost during training. All convolutional layers use rectified linear unit activations, apart from the last one that uses a sigmoid activation to produce the final output probabilities.

(295-08;2016/103) and Odense University (3-3013-1692/1; S-20120047) and with the 1964 Helsinki declaration and its later amendments or comparable ethical standards.

2.3 | Imaging

The PET/CT scans were acquired with different integrated PET/CT systems. The Sahlgrenska University Hospital used a Siemens Biograph 64 Truepoint, Skåne University Hospital used a Philips Gemini TF, and Odense University Hospital used Discovery VCT, Discovery STE, Discovery RX, and Discovery 690. PET images were acquired 1–1.5 hr after an intravenous injection of ^{18}F -fluorocholine. The patients fasted for 6 hr prior to the administration of the tracer, and each patient received a dose of 4 MBq per kg body weight. Attenuation correction was based on the CT scan. The PET slice thickness was 3.27–4 mm. Low-dose CT scans (120 kV, 30–400 mAs, 512×512 matrix) were obtained from the base of the skull to the mid-thigh. The CT slice thickness was 3–5 mm. The Organ CNN was trained on CT scans obtained without contrast whereas the 320 of the 399 patients used to train and test the Detection CNN were obtained with intravenous and/or oral contrast agents.

2.4 | Manual annotations

The CNNs were trained with images and corresponding manual annotations. The Detection CNN used manually annotated lymph node lesions on the PET/CT scans of PCa patients. Two nuclear medicine specialists annotated the material; Reader A annotated all of the material and was blinded to if the patients were part of the training or test group, and Reader B annotated the material of the test group and was blinded to the annotations by Reader A and the AI-based tool.

The instruction was to annotate uptake greater than background PET activity and judged by the reader to be consistent with a lymph node lesion and the CT component of the PET/CT was considered in this judgment. Thus, the images were interpreted in the same way

as in clinical practice since no specific criteria for detection of lymph node lesions have been established.

The Organ CNN was trained using manually annotated bones (skull, mandible, vertebrae, sternum, scapulae, clavicles, humeri, ribs, hip bones and femurs) and soft tissue organs (brain, lungs, heart, aorta, liver, spleen, kidneys, prostate and urinary bladder) on CT scans.

A cloud-based annotation tool (RECOMIA, www.recomia.org) was used for the annotation tasks. The Organ CNN was developed as a basic segmentation tool of RECOMIA and has been used in different studies (Lindgren Belal et al., 2017; Polymeri et al., 2020; Trägårdh et al., 2020).

2.5 | AI model

As mentioned above, our AI model was based on two convolutional networks. The Organ CNN segments a number of different organs and inputs an organ mask to the Detection CNN. Additionally, the Detection CNN also takes the CT and PET images as input (Figure 1). To simplify the structure, the PET image was resampled to the CT resolution.

Both networks use the same architecture which is described in Trägårdh et al., 2020, see Figure 2. The final convolutional layer of the Organ CNN has one channel per organ class with a softmax activation. For the Detection CNN, the final convolutional layer has a single output channel with sigmoid activation. For each voxel, the output value describes the estimated probability of that voxel belonging to a lymph node lesion.

2.5.1 | Training the Organ CNN

The organ CNN was trained on the 225 manually segmented CT scans from the organ data set using a negative log-likelihood loss. As typical in machine learning, the images were divided 80–20 into a training set used for direct parameter estimation and a validation set used to tune hyperparameters. Optimization was performed

using the Adam method with Nesterov momentum (Kingma & Adam, 2014). The learning rate was initialized to 0.0001 and reduced when the validation loss reached a plateau. After a few hours of training, the model was evaluated in the training group, and false positives were stored in a special group of hard examples that were sampled more frequently (10% of the samples) when the training was restarted.

2.5.2 | Training the Detection CNN

The lymph node lesions on the PET/CT scans manually annotated by Reader A were used for training. The Detection CNN was trained in the same way as the Organ CNN with one important difference. Since detection rather than the exact delineation of lymph node lesions is the focus of the AI-based tool, mimicking the exact boundaries of the annotations was not relevant. Thus, any voxels within 10 mm of the annotated metastases were marked as “don't care.” This means that when computing the loss functions, there was no loss for these voxels regardless of the output label. For the remaining voxels, the standard negative log-likelihood loss was used. Naturally, this leads to a slight oversegmentation of the metastases. As detection was the main goal, this was considered acceptable.

2.6 | Statistical methods

The agreement between Readers A and B in classifying patients with and without lymph node lesions was evaluated using kappa values. The significance of a difference in true positive detection between the AI-based tool and Reader A/B was evaluated using McNemar's test.

Associations among the number of automatically detected lymph node lesions, number of manually detected lymph node lesions, age, PSA, curative treatment and PCa-specific survival were investigated using a univariate Cox proportional hazards regression model. Survival time was calculated from the date of the PET/CT scan. Hazard ratios (HRs) and 95% confidence intervals (CIs) were estimated. The level of significance was set at 0.05.

3 | RESULTS

The agreement was good between the two readers who independently classified the 80 cases of the test group as positive or negative for the presence of lymph node lesions. In 18 of the 80 patients, both readers detected at least one lymph node lesion, and in 53 patients, they agreed that no lesion was present. The inter-reader reliability, as measured by the kappa value, was 0.72 (95% confidence interval 0.56–0.89). Reader A detected 117 lesions in the test group and the AI-based tool detected 98 (84%) and Reader B 87 (74%) of these lesions ($p = .045$). Reader B detected 111 lesions and the AI-based tool detected 90 (81%) and Reader A 87 (78%) of these lesions

TABLE 1 Univariate survival analysis demonstrating the associations among age, PSA, curative treatment, number of detected lymph nodes (auto/manual) and PCa-specific survival ($n = 79$)

	Hazard ratio	95% CI	p-Value
Age (years)	0.90	0.78–1.05	.19
PSA (ng/ml)	1.02	1.003–1.04	.02
Curative treatment	0.16	0.03–0.82	.03
Number of lymph nodes—Auto	1.19	1.05–1.33	.005
Number of lymph nodes—Reader A	1.46	1.18–1.80	.0005
Number of lymph nodes—Reader B	1.14	1.03–1.26	.01

($p = .63$). The AI-based tool detected one or more lymph node lesion in 71 of the 80 patients and classified only nine patients as negative for the presence of lymph node lesions. The agreement between the readers and the AI-based tool on a patient-by-patient level resulted therefore in low kappa values (0.08 and 0.11).

A total of 87 lymph node lesions were detected by both readers. The AI-based tool detected 80 of these lesions (92%). Fifty-four lesions were detected by one of the two readers only, with the AI-based tool detecting 28 of these lesions (52%). The AI-based tool made 219 detections not detected by any of the readers, corresponding to 2.7 detections per patient. Most of these detections represented activity in lymph nodes not classified as abnormal by the readers (46%) or in the intestines (25%). In total, the AI-based tool made 327 detections, of which 108 (33%) were classified as lymph node lesions by at least one of the two readers.

Eight patients in the test group died during the follow-up due to PCa. Their median survival time was 5.1 years (range 1.4–7.0). The follow-up time for the remaining 67 patients was 5.2 years (range 0.5–9.4). One patient was excluded from this analysis due to missing follow-up data. In the univariate Cox analysis, PSA, curative treatment and number of lymph node lesions detected by Reader A, Reader B and the AI-based tool were significantly associated with PCa-specific survival. The results are shown in Table 1.

4 | DISCUSSION

The results of this study show that an AI-based tool can be trained to automatically detect lymph node lesions on PET/CT with sensitivity comparable with that of two experienced readers. Furthermore, the number of detected lesions was significantly associated with PCa-specific survival. The main clinical application for this type of AI-based tool in combination with corresponding tools for the automated quantification of tumour burden in the prostate gland and skeleton would be to perform a comprehensive, fast, automated and objective analysis and provide a global disease score for patients with PCa.

Giovacchini and colleagues showed that ^{11}C -choline PET/CT predicts PCa-specific survival (Giovacchini et al., 2019). In their study, the PET/CT scans were visually interpreted as positive or negative, whereas AI-based tools can provide quantitative assessments of the tumour burden. Additional clinical information is most likely obtained from quantitative assessments of tumour burden compared with simply classifying the scans as “positive” or “negative.” The addition of improved reproducibility compared to interpretations by various physicians and significantly reduced reading times by directly highlighting possible true detections shows that the clinical benefit of the AI-based approach is even more apparent.

Our results illustrate the inter-observer variability associated with the detection of lymph node metastases and that an AI-based tool performs at least as well as an experienced nuclear medicine specialist in reproducing other specialists' detections. Considerable inter-reader variability in the interpretation of PET/CT scans has been reported. For example, Kluge et al. had five nuclear medicine experts with special expertise in PET/CT imaging of Hodgkin's lymphoma score interim PET/CT scans of 100 patients, which resulted in an inter-reader kappa value as low as 0.42 (Kluge et al., 2016), demonstrating the need for much more reliable and reproducible analysis methods.

The main limitation to the sensitivity of PET/CT scans for lymph node lesion detection is that an estimated 150–300 million metastatic cells need be present to be detected by PET (Alavi et al., 2019); thus, theoretically, micro-metastases will be missed by this technique. Arguably, deep histological analyses could detect the micro-metastases missed by PET/CT. However, performing these analyses on a routine basis would greatly increase the associated costs and time needed, since histopathologic examinations of lymph nodes normally comprise only 1%–2% of the relevant lymphatic tissue (Engvad et al., 2014).

Our study demonstrated the feasibility of using AI-based methods for the detection of lymph node lesions using choline-based tracers. However, as stated earlier, PSMA is a more sensitive tracer than choline, and these choline tracers are therefore being phased out in favour of PSMA-associated tracers (Ghafoor et al., 2019; Hope et al., 2019). There are differences in physiological uptake between choline and PSMA that need to be considered, but the similarities in the process to detect lymph nodes with high tracer uptake are very similar, and the organ masks trained by different CNNs would be the same for both tracers. It is therefore likely that CNNs can be trained to detect lymph node lesions based on training sets consisting of PSMA PET/CT scans.

We realize that only one nuclear medicine specialist and a limited training group were used to train our AI-based tool in our study. The good results in the separate test set show the feasibility of using AI-based tools for this type of image analysis and larger training groups with a more elaborated gold standard would most likely result in an even better AI-based tool. It should also be noted that the AI-based tool managed to handle PET/CT studies acquired with different cameras at different hospitals, indicating that it will be possible to develop AI-based tools that can be widely used irrespective of the clinical setting. Furthermore the Organ CNN was trained using

CT studies without contrast while 80% of the CT studies of the Detection CNN were acquired with contrast. The performance of the AI-based tool would most likely improve if CT studies with contrast also were used to train the Organ CNN.

A weakness of the study was that the performance of the tool in the test group was compared to readings of two nuclear medicine specialists and not to histopathologic findings. Nevertheless, we were able to demonstrate that the number of lymph node lesions detected by the AI-based tool was significantly associated with PCa-specific survival despite only a few terminal events. The AI-based made false detections for example representing activity in the intestines. This problem will be addressed in future development or our tool.

5 | CONCLUSION

We have shown that an AI-based tool can be trained to automatically detect lymph node metastases on PET/CT with sensitivity comparable with that of two experienced readers and that the number of detected lesions was significantly associated with PCa-specific survival. Future work will include efforts to decrease the rate of false detections by the tool, but this is a first step in the development towards clinically useful AI-based tools that can provide comprehensive and objective assessments of tumour burden in PCa patients based on PET/CT.

ACKNOWLEDGMENTS

This study was financed by grants from the Swedish state under the agreement between the Swedish government and the county councils and the ALF agreement (ALFGBG-720751) and by grants from EXINI Diagnostics AB (Lund, Sweden).

CONFLICT OF INTEREST

All authors declare that they have no conflicts of interest.

ORCID

Pablo Borrelli  <https://orcid.org/0000-0002-1665-7088>

Måns Larsson  <https://orcid.org/0000-0003-3137-1405>

Johannes Ulén  <https://orcid.org/0000-0003-1625-8367>

Olof Enqvist  <https://orcid.org/0000-0002-7456-1009>

Elin Trägårdh  <https://orcid.org/0000-0002-7116-303X>

Mads Hvid Poulsen  <https://orcid.org/0000-0002-7622-8402>

Mike Allan Mortensen  <https://orcid.org/0000-0002-7065-9623>

Henrik Kjölhede  <https://orcid.org/0000-0001-6441-4729>

Poul Flemming Høiland-Carlsen  <https://orcid.org/0000-0001-7420-2367>

<https://orcid.org/0000-0001-7420-2367>

Lars Edenbrandt  <https://orcid.org/0000-0002-0263-8820>

REFERENCES

- Alavi, A., Carlin, S. D., Werner, T. J., & Al-Zaghal, A. (2019). Suboptimal sensitivity and specificity of PET and other gross imaging techniques in assessing lymph node metastasis. *Molecular Imaging and Biology*, 21, 808–811. <https://doi.org/10.1007/s11307-018-01311-4>

- Armstrong, A. J., Anand, A., Edenbrandt, L., Bondesson, E., Bjartell, A., Widmark, A., Sternberg, C. N., Pili, R., Tuveson, H., Nordle, Ö., Carducci, M. A., & Morris, M. J. (2018). Phase 3 assessment of the automated bone scan index as a prognostic imaging biomarker of overall survival in men with metastatic castration-resistant prostate cancer: A secondary analysis of a randomized clinical trial. *JAMA Oncology*, *4*, 944–951. <https://doi.org/10.1001/jamaoncol.2018.1093>
- Eiber, M., Herrmann, K., Calais, J., Hadaschik, B., Giesel, F. L., Hartenbach, M., Hope, T., Reiter, R., Maurer, T., Weber, W. A., & Fendler, W. P. (2018). Prostate cancer molecular imaging standardized evaluation (PROMISE): Proposed miTNM classification for the interpretation of PSMA-ligand PET/CT. *Journal of Nuclear Medicine*, *59*, 469–478. <https://doi.org/10.2967/jnumed.117.198119>
- Engvad, B., Poulsen, M. H., Staun, P. W., Walter, S., & Marcussen, N. (2014). Histological step sectioning of pelvic lymph nodes increases the number of identified lymph node metastases. *Virchows Archiv*, *464*, 45–52. <https://doi.org/10.1007/s00428-013-1510-5>
- Fendler, W. P., Eiber, M., Beheshti, M., Bomanji, J., Ceci, F., Cho, S., Giesel, F., Haberkorn, U., Hope, T. A., Kopka, K., Krause, B. J., Mottaghy, F. M., Schöder, H., Sunderland, J., Wan, S., Wester, H.-J., Fanti, S., & Herrmann, K. (2017). 68 Ga-PSMA PET/CT: Joint EANM and SNMMI procedure guideline for prostate cancer imaging: Version 1.0. *European Journal of Nuclear Medicine and Molecular Imaging*, *44*, 1014–1024. <https://doi.org/10.1007/s00259-017-3670-z>
- Giovacchini, G., Guglielmo, P., Mapelli, P., Incerti, E., Gajate, A. M., Giovannini, E., Riondato, M., Briganti, A., Gianolli, L., Ciarmiello, A., & Picchio, M. (2019). 11 C-choline PET/CT predicts survival in prostate cancer patients with PSA < 1 NG/ml. *European Association of Nuclear Medicine*, *46*, 921–929.
- Høilund-Carlsen, P. F., Edenbrandt, L., & Alavi, A. (2019). Global disease score (GDS) is the name of the game!. *European Journal of Nuclear Medicine and Molecular Imaging*, *46*(9), 1768–1772. <https://doi.org/10.1007/s00259-019-04383-8>
- Kingma, D. P., & Ba, J. (2014). A method for stochastic optimization. *arXiv preprint arXiv:1412.6980*.
- Kjölhede, H., Almquist, H., Lyttkens, K., & Bratt, O. (2018). Pre-treatment 18 F-choline PET/CT is prognostic for biochemical recurrence, development of bone metastasis, and cancer specific mortality following radical local therapy of high-risk prostate cancer. *European Journal of Hybrid Imaging*, *2*, 16. <https://doi.org/10.1186/s41824-018-0034-2>
- Kluge, R., Chavdarova, L., Hoffmann, M., Kobe, C., Malkowski, B., Montravers, F., Kurch, L., Georgi, T., Dietlein, M., Wallace, W. H., Karlen, J., Fernández-Teijeiro, A., Cepelova, M., Wilson, L., Bergstraesser, E., Sabri, O., Mauz-Körholz, C., Körholz, D., & Hasenclever, D. (2016). Inter-reader reliability of early FDG-PET/CT response assessment using the Deauville scale after 2 cycles of intensive chemotherapy (OEPA) in Hodgkin's lymphoma. *PLoS One*, *11*(3), e0149072. <https://doi.org/10.1371/journal.pone.0149072>
- Lindgren Belal, S., Sadik, M., Kaboteh, R., Hasani, N., Enqvist, O., Svärm, L., Kahl, F., Simonsen, J., Poulsen, M. H., Ohlsson, M., Høilund-Carlsen, P. F., Edenbrandt, L., & Trägårdh, E. (2017). 3D skeletal uptake of 18F sodium fluoride in PET/CT images is associated with overall survival in patients with prostate cancer. *EJNMMI Research*, *7*, 15. <https://doi.org/10.1186/s13550-017-0264-5>
- Mortensen, M. A., Borrelli, P., Poulsen, M. H., Gerke, O., Enqvist, O., Ulén, J., Trägårdh, E., Constantinescu, C., Edenbrandt, L., Lund, L., & Høilund-Carlsen, P. F. (2019). Artificial intelligence-based versus manual assessment of prostate cancer in the prostate gland: A method comparison study. *Clinical Physiology and Functional Imaging*, *39*, 399–406. <https://doi.org/10.1111/cpf.12592>
- Polymeri, E., Sadik, M., Kaboteh, R., Borrelli, P., Enqvist, O., Ulén, J., Ohlsson, M., Trägårdh, E., Poulsen, M. H., Simonsen, J. A., Høilund-Carlsen, P. F., Johnsson, Å. A., & Edenbrandt, L. (2020). Deep learning-based quantification of PET/CT prostate gland uptake: Association with overall survival. *Clinical Physiology and Functional Imaging*, *40*, 106–113. <https://doi.org/10.1111/cpf.12611>
- Poulsen, M. H., Petersen, H., Høilund-Carlsen, P. F., Jakobsen, J. S., Gerke, O., Karstoft, J., Steffansen, S. I., & Walter, S. (2014). Spine metastases in prostate cancer: Comparison of technetium-99m-MDP whole-body bone scintigraphy, [18 F] choline positron emission tomography (PET)/computed tomography (CT) and [18 F] NaF PET/CT. *BJU International*, *114*, 818–823.
- Trägårdh, E., Borrelli, P., Kaboteh, R., Gillberg, T., Ulén, J., Enqvist, O., & Edenbrandt, L. (2020). RECOMIA—a cloud-based platform for artificial intelligence research in nuclear medicine and radiology. *EJNMMI Physics*, *7*, 1–2. <https://doi.org/10.1186/s40658-020-00316-9>

How to cite this article: Borrelli P, Larsson M, Ulén J, et al. Artificial intelligence-based detection of lymph node metastases by PET/CT predicts prostate cancer-specific survival. *Clin Physiol Funct Imaging*. 2020;00:1–6. <https://doi.org/10.1111/cpf.12666>